Stem Cell Reports
Report
OPEN ACCESS

Stepwise Differentiation of Pluripotent Stem Cells into Osteoblasts Using Four Small Molecules under Serum-free and Feeder-free Conditions

Kosuke Kanke,[1,2] Hideki Masaki,[6,7] Taku Saito,[2,4] Yuske Komiyama,[5] Hironori Hojo,[1] Hiromitsu Nakauchi,[6,7] Alexander C. Lichtler,[8] Tsuyoshi Takato,[2] Ung-il Chung,[1,3] and Shinsuke Ohba[1,3,*]
[1]Center for Disease Biology and Integrative Medicine
[2]Department of Sensory and Motor System Medicine
[3]Department of Bioengineering
[4]Department of Bone and Cartilage Regenerative Medicine
[5]Intensive Care Unit
The University of Tokyo, Tokyo 113-0033, Japan
[6]Japan Science Technology Agency, ERATO, Nakauchi Stem Cell and Organ Regeneration Project
[7]Division of Stem Cell Therapy, Center for Stem Cell Biology and Regenerative Medicine, Institute of Medical Science
The University of Tokyo, Tokyo 108-8639, Japan
[8]Department of Reconstructive Sciences, School of Dental Medicine, University of Connecticut Health Center, Farmington, CT 06030, USA
*Correspondence: ohba@bioeng.t.u-tokyo.ac.jp
http://dx.doi.org/10.1016/j.stemcr.2014.04.016

SUMMARY

Pluripotent stem cells are a promising tool for mechanistic studies of tissue development, drug screening, and cell-based therapies. Here, we report an effective and mass-producing strategy for the stepwise differentiation of mouse embryonic stem cells (mESCs) and mouse and human induced pluripotent stem cells (miPSCs and hiPSCs, respectively) into osteoblasts using four small molecules (CHIR99021 [CHIR], cyclopamine [Cyc], smoothened agonist [SAG], and a helioxanthin-derivative 4-(4-methoxyphenyl)pyrido[4′,3′:4,5]thieno [2,3-b]pyridine-2-carboxamide [TH]) under serum-free and feeder-free conditions. The strategy, which consists of mesoderm induction, osteoblast induction, and osteoblast maturation phases, significantly induced expressions of osteoblast-related genes and proteins in mESCs, miPSCs, and hiPSCs. In addition, when mESCs defective in runt-related transcription factor 2 (*Runx2*), a master regulator of osteogenesis, were cultured by the strategy, they molecularly recapitulated osteoblast phenotypes of *Runx2* null mice. The present strategy will be a platform for biological and pathological studies of osteoblast development, screening of bone-augmentation drugs, and skeletal regeneration.

INTRODUCTION

The limited number of osteoblasts that can be obtained from animals hinders the performance of extensive studies on protein interactions, transcriptional networks, and epigenetics in osteoblast development. Therefore, pluripotent stem cell-based osteogenic differentiation may be an attractive model for such studies, given the pluripotency and capacity for self-renewal of stem cells. Although several strategies have been used to differentiate pluripotent stem cells, including embryonic stem cells (ESCs) and induced pluripotent stem cells (iPSCs) into osteoblasts (Bilousova et al., 2011; Buttery et al., 2001; Li et al., 2010; Kao et al., 2010; Kawaguchi et al., 2005; Phillips et al., 2001; Tai et al., 2004; Ye et al., 2011; zur Nieden et al., 2003), none of these is a stepwise differentiation strategy that uses small molecule inducers and serum-free monolayer cultures without the formation of embryoid bodies (EBs).

Using the combination of a mitogen-activated protein kinase kinase (MEK) inhibitor, PD0325901 (PD03), and a glycogen synthase kinase 3 (GSK3) inhibitor, CHIR99021 (CHIR), which will hereafter be referred to as 2i, mouse ESCs (mESCs) are maintained in a ground state (Ying et al., 2008). CHIR activates canonical Wnt signaling by suppressing the degradation of β-catenin (Bain et al., 2007). Canonical Wnt signaling cues also specify the differentiation of germ layers and multipotent stem cells into mesodermal cells (Davis and Zur Nieden, 2008). We recently described the gene regulatory networks underlying canonical Wnt signaling-mediated control of mesoderm differentiation and pluripotency in mESCs (Zhang et al., 2013).

The formation of osteoblasts is a sequential process. In mesoderm-derived skeletons, cells in the lateral plate mesoderm or the paraxial mesoderm give rise to skeletal progenitors, which then differentiate into bone-forming osteoblasts and cartilage-forming chondrocytes (Akiyama et al., 2005). We and others have shown that hedgehog (Hh) signaling is essential for normal osteoblast development, particularly for the specification of osteo-chondroprogenitors into osteoblast precursors, which express runt-related transcription factor 2 (*Runx2*), a transcription factor essential for bone formation (Hojo et al., 2012; Long et al., 2004; St-Jacques et al., 1999); the smoothened (SMO) agonist (SAG), a Hh signaling activator, promoted early osteoblast differentiation in perichondrial cells, which consist of osteo-chondroprogenitors (Hojo et al., 2012). This finding suggested that SAG could efficiently

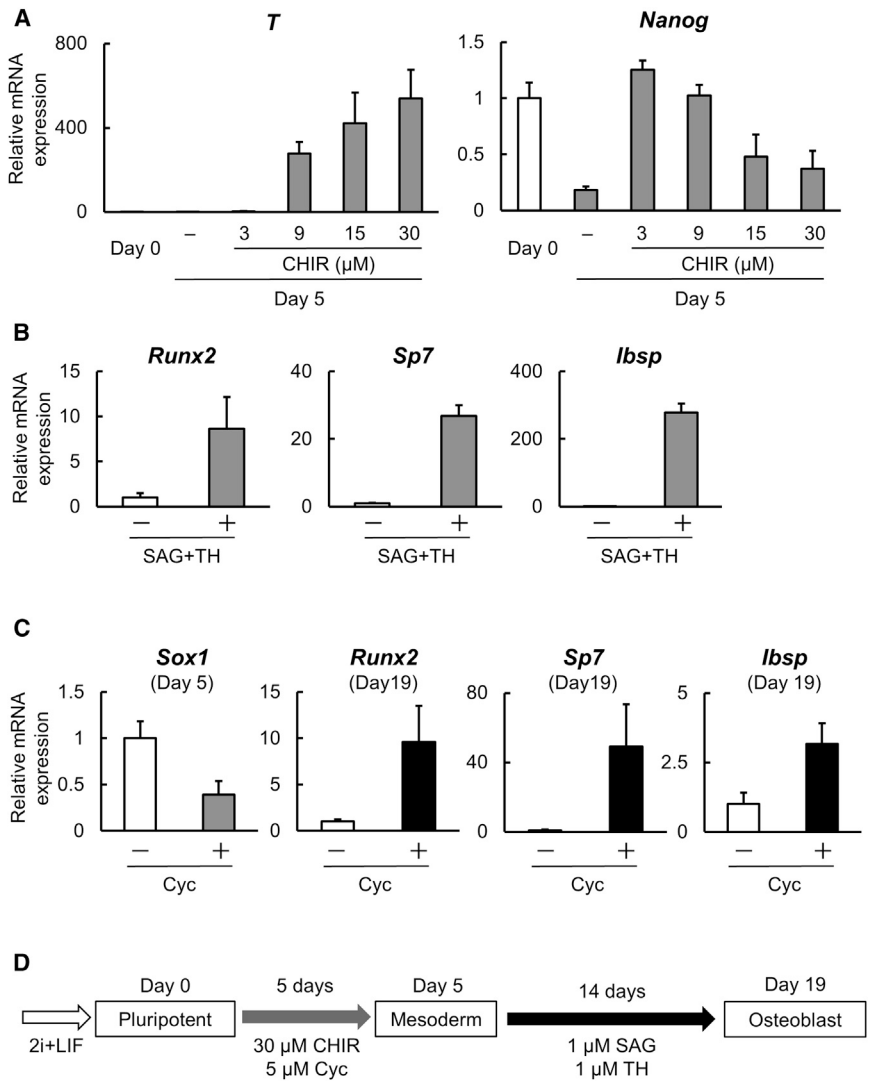

Figure 1. Optimization of Mesoderm Induction and Osteoblast Induction in mESCs

(A) The effect of the 5-day treatment with CHIR on mesoderm differentiation and the suppression of the pluripotent state in mESCs. 2i-cultured mESCs were treated for 5 days with CHIR at different concentrations. The mRNA expression levels were determined using RT-quantitative PCR (RT-qPCR). The data are expressed as the mean ± SEM from three independent experiments. See also Figure S1.

(B) The effect of the 14-day treatment with SAG plus TH on osteoblast differentiation of mESC-derived mesodermal cells. The mESCs were cultured with 30 μM CHIR for 5 days, then with (gray bars) or without (white bars) 1 μM SAG and 1 μM TH for an additional 14 days. The mRNA expression was determined using RT-qPCR. The data are expressed as the mean ± SEM from four independent experiments.

(C) The effect of Cyc on mesoderm induction and subsequent osteoblast induction in mESCs. mESCs were cultured with 30 μM CHIR for 5 days in the presence or absence of 5 μM Cyc and treated for 14 days with SAG plus TH. The mRNA expression was determined using RT-qPCR on days 5 and 19, respectively. The data are expressed as the mean ± SEM from four independent experiments.

(D) A schematic showing the three-phase strategy for osteoblast differentiation from mESCs using the four small molecules under chemically defined conditions.

differentiate mesodermal cells into osteoblast precursors. Moreover, it also indicated that SAG alone might not be sufficient to direct the differentiation of these precursors into mature osteoblasts. In terms of molecules inducing osteoblast maturation, we identified the helioxanthin-derivative 4-(4-methoxyphenyl)pyrido[4′,3′:4,5]thieno[2,3-b]pyridine-2-carboxamide (TH) as an osteogenic small molecule that acts on preosteoblasts in a bone morphogenetic protein (BMP)-dependent manner (Ohba et al., 2007b). Furthermore, we recently reported the combinatorial effect of SAG and TH on the differentiation of mesenchymal cells into osteoblasts (Maeda et al., 2013).

Based on these findings, we hypothesized that pluripotent stem cells could be efficiently differentiated into osteoblasts under defined conditions by sequentially treating the cells with the above-mentioned small molecules in an appropriate manner. The present study was designed to establish a stepwise differentiation protocol for osteoblast differentiation from pluripotent stem cells by utilizing the small molecule inducers under serum-free and feeder-free conditions.

RESULTS AND DISCUSSION

We initially attempted to differentiate 2i-cultured mESCs into mesodermal cells by activating canonical Wnt signaling with CHIR in 2i culture media. CHIR upregulated the mesoderm-related genes *T* and *Mixl1* in a dose-dependent manner relative to day 0 (Figure 1A; Figure S1A available online). The expression of the pluripotency-related genes *Nanog*, *Pou5f1*, and *Sox2* was suppressed in cells treated with high concentrations of CHIR relative to day 0 (Figures 1A and S1A). In addition, the expression of

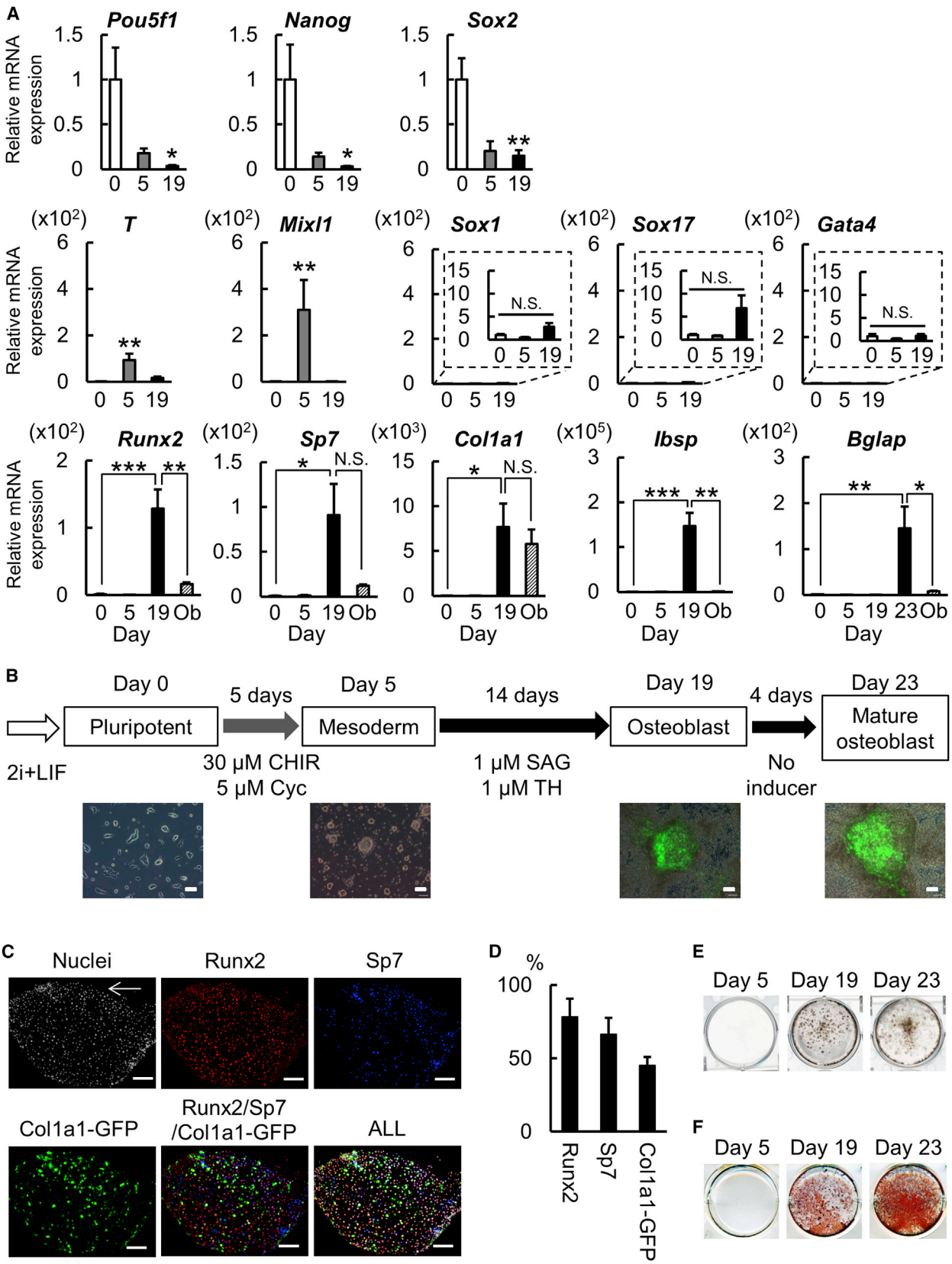

(legend on next page)

T was higher on day 5 than on day 7, and higher expression of the mesoderm-related genes was associated with higher expression of osteoblast-related genes in subsequent osteoblast induction (Figure S1B). Therefore, we selected the 5-day treatment protocol using 30 μM CHIR for the mesoderm induction of mESCs. To induce osteoblast differentiation of the mESC-derived mesoderm cells, we then cultured them in 2i culture media containing 1 μM SAG, 1 μM TH, and other osteogenic supplements (Jaiswal et al., 1997). *Runx2*, *Sp7*, and *Ibsp* were upregulated following treatment for 2 weeks with SAG plus TH relative to the control group (Figure 1B). Thus, the stepwise differentiation from mESCs into osteoblasts via mesoderm formation was achieved using the three small molecules CHIR, SAG, and TH.

Given the roles of Hh signaling during the development of the CNS (Martí and Bovolenta, 2002), recombinant Hh proteins or SAGs have been used to differentiate pluripotent stem cells into motor neurons (Nizzardo et al., 2010). Moreover, 2i-cultured ESCs preferentially differentiate into ectoderm lineages rather than mesoderm lineages (Marks et al., 2012). These findings led us to examine whether the suppression of Hh signaling during the mesoderm induction would block neuro-ectoderm specification, resulting in enhanced osteoblast differentiation. The combinatorial use of the Hh signaling inhibitor cyclopamine (Cyc) and CHIR during the 5-day mesoderm induction induced the downregulation of *Sox1* on day 5 and led to increased osteoblast differentiation (Figure 1C).

As shown in Figure 1D, we propose an optimized strategy for promoting osteoblast differentiation from mESCs under chemically defined conditions. This strategy consists of three phases: the maintenance of mESCs using 2i plus leukemia inhibitory factor (LIF) culture, mesoderm induction by CHIR in combination with Cyc-mediated suppression of neuro-ectoderm differentiation, and osteoblast induction by SAG and TH. Given that Cyc induces SMO translocation to the primary cilium despite its inhibitory effect on Hh signaling (Wang et al., 2009), the accumulated SMO in the cilium may result in increased sensitivity to subsequent SAG treatment, which may also contribute to the osteoblast differentiation by SAG and TH during the osteoblast induction phase. SAG and TH cooperatively induce osteoblast differentiation, possibly through SAG-mediated specification into an osteoblast lineage and TH-mediated promotion of late osteoblast differentiation (Hojo et al., 2013; Maeda et al., 2013; Ohba et al., 2007b).

Gene expression patterns in mESCs cultured according to this strategy are shown in Figure 2A. *Pou5f1*, *Nanog*, and *Sox2* were significantly downregulated on day 19, indicating that the mESCs gradually exited from the pluripotent state as differentiation progressed. *T* and *Mixl1* were upregulated by mesoderm induction (day 5) and in turn were downregulated by osteoblast induction (day 19). *Sox1*, *Sox17*, and *Gata4*, which are ectoderm and endoderm marker genes, were not altered throughout the culture. These data suggested that the present strategy specifically directs pluripotent cells toward a mesodermal cell fate. The osteoblast-related genes, *Runx2*, *Sp7*, *Col1a1*, and *Ibsp*, were upregulated during the osteoblast induction phase (day 19) relative to day 0; *Runx2*, *Sp7*, *Col1a1*, and *Ibsp* were upregulated approximately 128-, 91-, 7,680-, and 147,300-fold, respectively. However, the 19-day culture was not long enough for the cells to express *Bglap*, a bona fide marker of mature osteoblasts; culturing the cells for an additional 4 days in the absence of SAG or TH induced a 145-fold upregulation of *Bglap*.

Expressions of the osteoblast-related genes in the induced cells were higher than or comparable to those in cultured mouse primary osteoblasts (Figure 2A). Expressions of osteoblast-related transcription factors in the induced cells were comparable to those in freshly isolated mouse osteoblasts (fresh mObs), although the expressions of matrix genes in the induced cells were not as high as those in the fresh mObs (Figure S2A). When gene expressions were compared between the present strategy and an

Figure 2. Characterization of mESC-Derived Cells Generated Using the Present Strategy for Osteoblast Differentiation

(A) Expressions of pluripotency-related (*Pou5f1*, *Nanog*, and *Sox2*), mesoderm-related (*T* and *Mixl1*), ectoderm-related (*Sox1*), endoderm-related (*Sox17* and *Gata4*), and osteoblast-related genes (*Runx2*, *Sp7*, *Col1a1*, *Ibsp*, and *Bglap*) on days 0 (white bars), 5 (gray bars), 19, and 23 (black bars) and cultured calvarial osteoblasts isolated from mouse neonates (Ob; hatched bars). The *Sox1*, *Sox17*, and *Gata4* expression data are shown in the dotted rectangular box with the smaller scale of the y axis. The data are expressed as the mean ± SEM from eight independent experiments. *$p < 0.05$ versus day 0; **$p < 0.01$ versus day 0; ***$p < 0.001$ versus day 0; N.S., nonsignificant versus day 0. See also Figures S2A–S2C.

(B) A schematic showing the four-phase strategy for directing mESCs into mature osteoblasts. The lower panels indicate the morphology and expression of GFP in 2.3 kb Col1a1-GFP mESCs cultured according to the present strategy. Scale bars, 100 μm.

(C) Protein expressions of the osteoblast-related markers in 2.3 kb Col1a1-GFP mESCs cultured according to the present strategy on day 19. The arrow shows the surface of the cell cluster. Scale bars, 100 μm. Nuclei and SP7 are shown in pseudocolor. See also Figure S2D.

(D) Quantification of cells expressing osteoblast-related marker proteins. The data are expressed as the mean of percentages of cells positive for both DAPI and markers in total of DAPI-positive cells analyzed ± SEM from three independent experiments.

(E and F) von Kossa staining (E) and alizarin red staining (F) on days 5, 19, and 23 in mESCs cultured according to the present strategy.

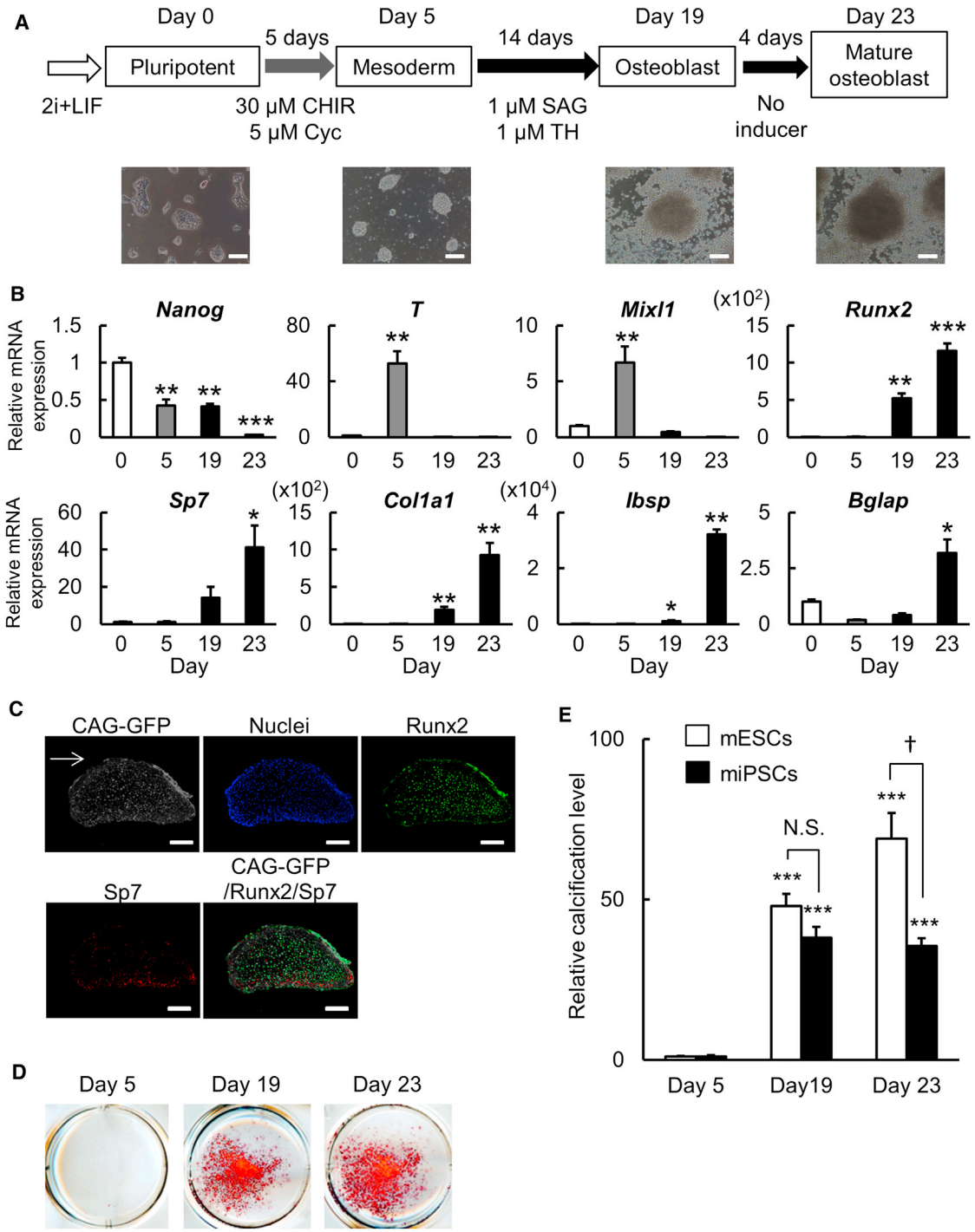

Figure 3. Differentiation of miPSCs into Osteoblasts

(A) A schematic showing the strategy for inducing osteoblast differentiation of miPSCs. The lower panels show the morphology of colonies of miPSCs and induced cells on days 0, 5, 19, and 23. Scale bars, 100 μm.

(B) Expressions of pluripotency-related (*Nanog*), mesoderm-related (*T* and *Mixl1*), and osteoblast-related genes (*Runx2*, *Sp7*, *Col1a1*, *Ibsp*, and *Bglap*) on days 0 (white bars), 5 (gray bars), 19, and 23 (black bars) in miPSCs. The data are expressed as the mean ± SEM from six independent experiments. *$p < 0.05$ versus day 0; **$p < 0.01$ versus day 0; ***$p < 0.001$ versus day 0.

(C) Protein expressions of the osteoblast-related markers in CAG-GFP miPSCs cultured according to the present strategy on day 23. RUNX2, SP7, and GFP are shown in pseudocolor. The arrow shows the surface of the cell cluster. Scale bars, 100 μm.

(legend continued on next page)

EB-based conventional one (Kawaguchi et al., 2005), the present strategy induced significantly lower expressions of *Sox17* and *Gata4* on day 19 and higher expressions of *Runx2*, *Sp7*, *Col1a1*, *Ibsp*, and *Bglap* on day 19 or 23 than the conventional method (Figure S2B). The present strategy is likely to differentiate mESCs into an osteoblast lineage more specifically than the conventional method, at least partly by avoiding their differentiation into unfavorable lineages. When we examined gene expressions at several time points during the culture (Figure S2C), the expression profile resembled a proposed model for the Hh signaling-mediated specification of skeletal progenitors into *Runx2*-positive osteoblast precursors and their subsequent differentiation into osteoblasts in skeletal development (Rodda and McMahon, 2006).

Thus, we established a strategy to direct mESCs toward a mature osteoblast cell fate by sequentially using four small molecules, CHIR, Cyc, SAG, and TH, under chemically defined conditions. This protocol involves the addition of a fourth osteoblast maturation phase to the three-phase strategy described earlier (Figure 2B). The effectiveness of the strategy was further confirmed by the expression of GFP on days 19 and 23 in mESCs engineered to express GFP under the control of an osteoblast-specific rat 2.3 kb *Col1a1* promoter (2.3 kb Col1a1-GFP mESCs) (Figure 2B) (Ohba et al., 2007a).

We used immunohistochemistry to measure the expression of RUNX2, SP7, and GFP in the induced 2.3 kb Col1a1-GFP mESCs. RUNX2, SP7, and the 2.3 kb Col1a1-GFP were highly expressed in the induced cells on day 19. RUNX2 and SP7 were colocalized in nuclei, and 2.3 kb Col1a1-GFP was largely observed in the cytoplasm and nuclei (Figure 2C). The average percentages of RUNX2-, SP7-, and GFP-positive cells were 78% ± 3%, 66% ± 5%, and 45% ± 1%, respectively (Figure 2D). The different percentages of those markers in our culture are consistent with the physiological process of osteoblast development. The percentages enable us to estimate the final yields of each osteoblastic population, given that 900,000 ± 150,000 cells/cm^2 were obtained on day 19 of the culture from 100,000 cells/cm^2 of input. Pluripotency markers were hardly expressed in the induced cells on day 19 (Figure S2D). The average percentages of OCT4-, NANOG-, and SOX2-positive cells were 2.3% ± 0.6%, 1.5% ± 0.7%, and 9.0% ± 3.1%, respectively (Figure S2D). In addition, BRACHYURY (T), a mesoderm maker, was ubiquitously expressed in the induced cells on day 5 (Figure S1C). von Kossa staining and alizarin red staining revealed the uniform formation of calcified cell clusters by days 19 and 23 (Figures 2E and 2F). These results indicate that the present strategy induced both the expression of osteoblast-related genes and the calcification of matrix, two key features of osteoblasts.

To confirm that the present strategy could be useful for investigating osteoblast development using gene-manipulated mESCs in vitro, we examined whether *Runx2*$^{-/-}$ mESCs cultured using the present strategy could molecularly recapitulate osteoblast phenotypes in *Runx2*$^{-/-}$ mice (Figure S3A). *Runx2*$^{-/-}$ mESCs showed similar transient upregulation of *T* to *Runx2*$^{+/+}$ mESCs, but *Sp7* and *Bglap* were hardly upregulated in *Runx2*$^{-/-}$ mESCs on day 19 compared to day 0 and day 5. Importantly, the expression of the early osteoblast marker gene *Ibsp* showed a 212-fold upregulation in *Runx2*$^{-/-}$ mESCs on day 19, although the level was lower than that observed in *Runx2*$^{+/+}$ mESCs. In alizarin red staining, the calcification level of *Runx2*$^{-/-}$ mESCs was lower than that of *Runx2*$^{+/+}$ ones on both days 19 and 23 (Figures 2F, S3B, and S3C). These observations were consistent with the bone phenotypes of *Runx2*$^{-/-}$ mice (Komori et al., 1997; Tu et al., 2012). Thus, the present strategy can at least partially recapitulate physiological osteoblast development and will be useful for analyzing osteoblast development using gene-manipulated ESCs in vitro.

Because the direct differentiation of mouse iPSCs (miPSCs) and human iPSCs (hiPSCs) into osteogenic cells has been previously reported by Bilousova et al. (2011), Kao et al. (2010), and Levi et al. (2012), we applied the present strategy to 2i-adapted miPSCs established from fibroblasts of mice expressing GFP (CAG-GFP miPSCs) (Okabe et al., 1997) (Figure 3A). *Nanog* was downregulated throughout the culture compared to day 0. *T* and *Mixl1* were transiently upregulated by mesoderm induction on day 5. The osteoblast-related genes *Runx2*, *Sp7*, *Col1a1*, *Ibsp*, and *Bglap* were upregulated by the osteoblast induction (Figure 3B). RUNX2 and SP7 proteins were highly expressed in the induced cells on day 23, and their signals were merged with that of GFP (Figure 3C), suggesting that CAG-GFP miPSCs were differentiated into cells expressing osteoblast-related proteins. Calcified cell clusters were formed on days 19 and 23 (Figure 3D). In the comparison of calcification levels between mESCs and miPSCs, both cell types were calcified at a similar level on day 19; mESCs then showed more calcification on day 23 (Figure 3E).

(D) Alizarin red staining on days 5, 19, and 23 in miPSCs cultured according to the present strategy.
(E) Alizarin red staining-based quantification of calcification levels in mESCs and miPSCs cultured according to the present strategy, relative to day 5 in each cell type. ***$p < 0.001$ versus day 5 in each cell type; N.S., nonsignificant; †$p < 0.05$. The data are expressed as the mean ± SEM from six independent experiments.

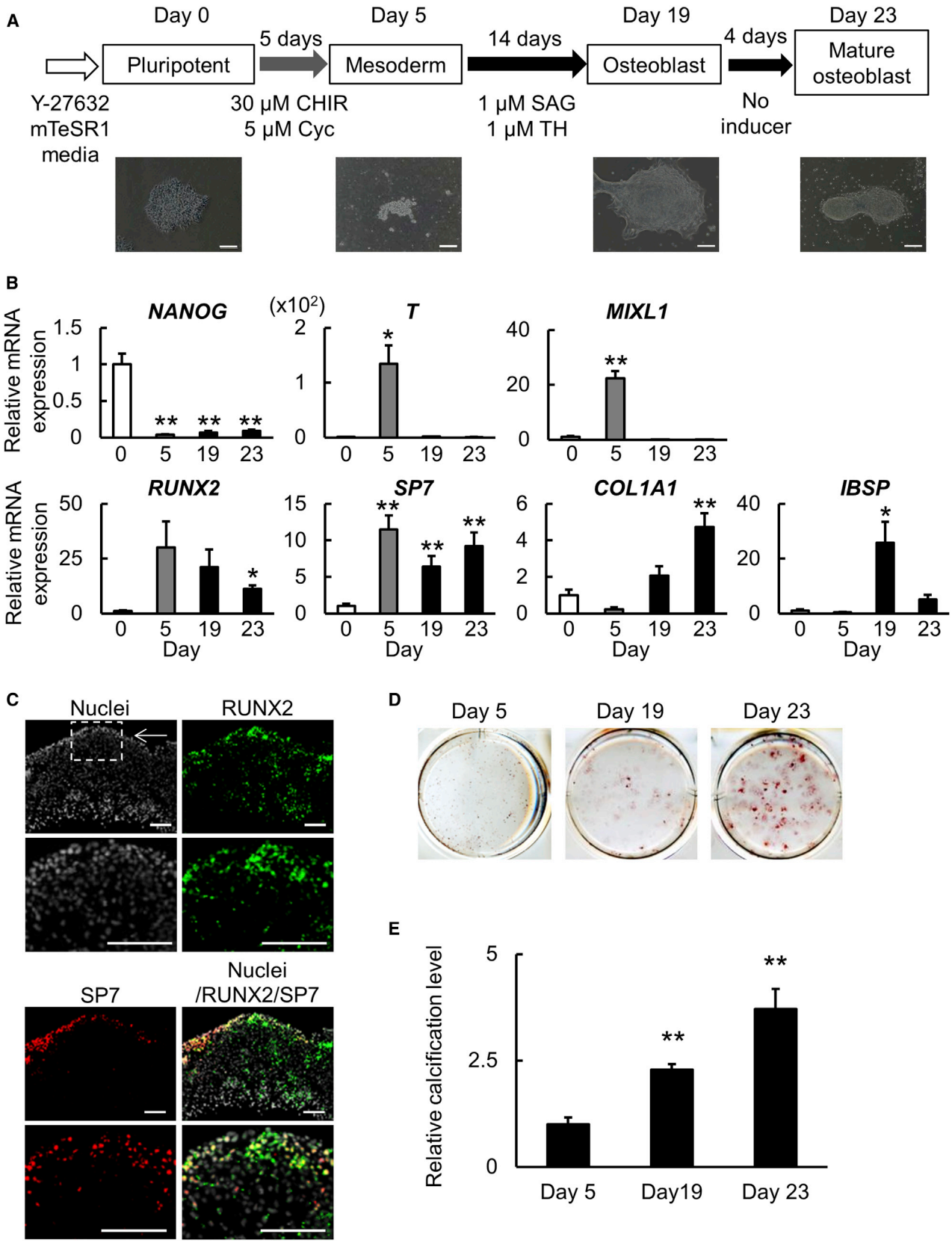

(legend on next page)

Thus, the present strategy efficiently differentiates both mESCs and miPSCs into osteoblasts by sequentially treating the cells with four small molecules, CHIR, Cyc, SAG, and TH, under chemically defined conditions.

Finally, we cultured hiPSCs according to the present strategy with some modifications (Figure 4A; Supplemental Experimental Procedures). hiPSCs formed colonies on day 0. In the mesoderm induction phase, these colonies were disrupted, but the cells generated some clusters upon CHIR and Cyc treatment. The remaining cells proliferated and formed colonies by days 19 and 23 of the osteoblast induction and maturation phases (Figure 4A). Gene expression patterns in the cultured hiPSCs are shown in Figure 4B. *NANOG* was downregulated during induction. *T* and *MIXL1* were transiently upregulated on day 5. *RUNX2* and *SP7* were also upregulated on day 5; their expression levels were maintained and statistically significant on day 23 compared with day 0. *IBSP* and *COL1A1* were significantly upregulated on days 19 and 23, respectively. The contribution of Hh signaling to osteoblast-related gene expression might cause differences in the gene expression pattern between human and mouse cells, as previously reported by Plaisant et al. (2009). On day 23, RUNX2 protein was evenly expressed in cell clusters, and SP7 was expressed in the periphery, where RUNX2 and SP7 were colocalized (Figure 4C). Calcification on days 19 and 23 was significantly higher than that on day 5 (Figures 4D and 4E). These results suggest that the present strategy is capable of differentiating hiPSCs into osteoblasts.

This study demonstrates the robust generation of osteoblasts from pluripotent stem cells using four small molecules under serum-free and feeder-free conditions. This strategy requires no or very little use of confounding factors derived from serum and feeder cells. Such a simple, small molecule-based system offers significant benefits for skeletal research and regenerative medicine by minimizing costs and maintaining the stability of the inducers. However, this study has two major limitations. First, the target molecules of TH are unclear; we are currently screening for these targets using a proteomic approach with a modified TH carrying a moiety that binds to magnetic beads via an amide bond. Second, we used Matrigel, which was not a fully defined reagent (Hughes et al., 2010), for hiPSCs to maintain cell viability. Because we observed a substantial level of hiPSC death on the Matrigel-coated plates during the initial 5-day induction, this strategy might be deleterious for the survival and differentiation of hiPSCs. In future studies, there will be a need for defined reagents suppressing the cell death of hiPSCs as well as reagents that will eliminate residual pluripotent cells (Ben-David and Benvenisty, 2011; Tang et al., 2011); the 2.3 kb Col1a1-GFP may be used to sort out osteoblasts. In conclusion, the present stepwise differentiation strategy offers a tool for in vitro mechanistic studies of osteoblast development and stem cell-based therapies for massive bone defects, although the strategy will need to be further optimized to enable broader application.

EXPERIMENTAL PROCEDURES

Differentiation of mESCs into Osteoblasts

mESCs were seeded at 100,000 cells/cm^2 in gelatin-coated 6-well plates and cultured for 24 hr in 2i culture media (see Supplemental Experimental Procedures) supplemented with CHIR (Wako Pure Chemical Industries, 039-20831; Axon Medchem, 1386), PD0325901 (Wako; 163-24001), and LIF (Millipore; ESG1107). After briefly washing the cells with PBS, the 5-day induction protocol was initiated to differentiate the cells toward a mesoderm lineage. 2i culture media without CHIR, PD0325901, or LIF were used as basal media during the differentiation culture and supplemented with small molecules for each differentiation step as shown below. The mesoderm induction was achieved by culturing the cells with 30 μM CHIR and 5 μM Cyc (Enzo Life Sciences; BML-GR334) in 2i culture media. To induce osteoblast differentiation, we then cultured the cells for 14 days in 2i culture media supplemented with 50 μg/ml ascorbic acid phosphate (AsAP) (Sigma-Aldrich; A4034), 10 mM β-glycerophosphate (β-GP) (Sigma-Aldrich; G9422), 0.1 μM dexamethasone (Dex) (Wako; 041-18861), 1 μM SAG (Calbiochem; 566660), and 1 μM TH (synthesized by Takeda Chemical Industries). For osteoblast maturation, the cells were cultured for an additional 4 days in 2i

Figure 4. Differentiation of hiPSCs into Osteoblasts

(A) A schematic showing the strategy for inducing osteoblast differentiation of hiPSCs. The lower panels show the morphology of colonies of hiPSCs and induced cells on days 0, 5, 19, and 23. Scale bars, 100 μm.

(B) Expressions of pluripotency-related (*NANOG*), mesoderm-related (*T* and *MIXL1*), and osteoblast-related genes (*RUNX2*, *SP7*, *COL1A1*, and *IBSP*) on days 0 (white bars), 5 (gray bars), 19, and 23 (black bars) in hiPSCs. The data are expressed as the mean ± SEM from six independent experiments. *$p < 0.05$ versus day 0; **$p < 0.01$ versus day 0.

(C) Protein expressions of RUNX2 and SP7 in hiPSCs on day 23. Lower panels show magnified views of the region marked by a dotted rectangular box in the left-upper panel. Nuclei are shown in pseudocolor. The arrow shows the surface of the cell cluster. Scale bars, 100 μm.

(D) Alizarin red staining on days 5, 19, and 23 in hiPSCs cultured according to the present strategy.

(E) Alizarin red staining-based quantification of calcification in hiPSCs cultured according to the present strategy, relative to that of day 5. **$p < 0.01$ versus day 5. The data are expressed as the mean ± SEM from six independent experiments.

culture media supplemented with AsAP, β-GP, and Dex. The culture media were replaced daily. TH can be distributed upon request.

SUPPLEMENTAL INFORMATION

Supplemental Information includes Supplemental Experimental Procedures, three figures, and two tables and can be found with this article online at http://dx.doi.org/10.1016/j.stemcr.2014.04.016.

ACKNOWLEDGMENTS

We thank Dr. M.J. Owen for his kind gift of the *Runx2* knockout ESCs and Dr. Andrew P. McMahon for his helpful input. This work was supported by Grants-in-Aid for Scientific Research (#23689079), the Center for Medical System Innovation, the Graduate Program for Leaders in Life Innovation, Core-to-Core Program A (Advanced Research Networks), the Funding Program for World-Leading Innovative R&D on Science and Technology, the Center for NanoBio Integration, the S-innovation program, Nakayama Foundation for Human Science and the Nakatomi Foundation Research Grant.

Received: July 9, 2013
Revised: April 24, 2014
Accepted: April 28, 2014
Published: May 22, 2014

REFERENCES

Akiyama, H., Kim, J.E., Nakashima, K., Balmes, G., Iwai, N., Deng, J.M., Zhang, Z., Martin, J.F., Behringer, R.R., Nakamura, T., and de Crombrugghe, B. (2005). Osteo-chondroprogenitor cells are derived from Sox9 expressing precursors. Proc. Natl. Acad. Sci. USA *102*, 14665–14670.

Bain, J., Plater, L., Elliott, M., Shpiro, N., Hastie, C.J., McLauchlan, H., Klevernic, I., Arthur, J.S.C., Alessi, D.R., and Cohen, P. (2007). The selectivity of protein kinase inhibitors: a further update. Biochem. J. *408*, 297–315.

Ben-David, U., and Benvenisty, N. (2011). The tumorigenicity of human embryonic and induced pluripotent stem cells. Nat. Rev. Cancer *11*, 268–277.

Bilousova, G., Jun, H., King, K.B., De Langhe, S., Chick, W.S., Torchia, E.C., Chow, K.S., Klemm, D.J., Roop, D.R., and Majka, S.M. (2011). Osteoblasts derived from induced pluripotent stem cells form calcified structures in scaffolds both in vitro and in vivo. Stem Cells *29*, 206–216.

Buttery, L.D.K., Bourne, S., Xynos, J.D., Wood, H., Hughes, F.J., Hughes, S.P.F., Episkopou, V., and Polak, J.M. (2001). Differentiation of osteoblasts and in vitro bone formation from murine embryonic stem cells. Tissue Eng. *7*, 89–99.

Davis, L.A., and Zur Nieden, N.I. (2008). Mesodermal fate decisions of a stem cell: the Wnt switch. Cell. Mol. Life Sci. *65*, 2658–2674.

Hojo, H., Ohba, S., Yano, F., Saito, T., Ikeda, T., Nakajima, K., Komiyama, Y., Nakagata, N., Suzuki, K., Takato, T., et al. (2012). Gli1 protein participates in Hedgehog-mediated specification of osteoblast lineage during endochondral ossification. J. Biol. Chem. *287*, 17860–17869.

Hojo, H., Ohba, S., Taniguchi, K., Shirai, M., Yano, F., Saito, T., Ikeda, T., Nakajima, K., Komiyama, Y., Nakagata, N., et al. (2013). Hedgehog-Gli activators direct osteo-chondrogenic function of bone morphogenetic protein toward osteogenesis in the perichondrium. J. Biol. Chem. *288*, 9924–9932.

Hughes, C.S., Postovit, L.M., and Lajoie, G.A. (2010). Matrigel: a complex protein mixture required for optimal growth of cell culture. Proteomics *10*, 1886–1890.

Jaiswal, N., Haynesworth, S.E., Caplan, A.I., and Bruder, S.P. (1997). Osteogenic differentiation of purified, culture-expanded human mesenchymal stem cells in vitro. J. Cell. Biochem. *64*, 295–312.

Kao, C.L., Tai, L.K., Chiou, S.H., Chen, Y.J., Lee, K.H., Chou, S.J., Chang, Y.L., Chang, C.M., Chen, S.J., Ku, H.H., and Li, H.Y. (2010). Resveratrol promotes osteogenic differentiation and protects against dexamethasone damage in murine induced pluripotent stem cells. Stem Cells Dev. *19*, 247–258.

Kawaguchi, J., Mee, P.J., and Smith, A.G. (2005). Osteogenic and chondrogenic differentiation of embryonic stem cells in response to specific growth factors. Bone *36*, 758–769.

Komori, T., Yagi, H., Nomura, S., Yamaguchi, A., Sasaki, K., Deguchi, K., Shimizu, Y., Bronson, R.T., Gao, Y.H., Inada, M., et al. (1997). Targeted disruption of Cbfa1 results in a complete lack of bone formation owing to maturational arrest of osteoblasts. Cell *89*, 755–764.

Levi, B., Hyun, J.S., Montoro, D.T., Lo, D.D., Chan, C.K., Hu, S., Sun, N., Lee, M., Grova, M., Connolly, A.J., et al. (2012). In vivo directed differentiation of pluripotent stem cells for skeletal regeneration. Proc. Natl. Acad. Sci. USA *109*, 20379–20384.

Li, F., Bronson, S., and Niyibizi, C. (2010). Derivation of murine induced pluripotent stem cells (iPS) and assessment of their differentiation toward osteogenic lineage. J. Cell. Biochem. *109*, 643–652.

Long, F.X., Chung, U.I., Ohba, S., McMahon, J., Kronenberg, H.M., and McMahon, A.P. (2004). Ihh signaling is directly required for the osteoblast lineage in the endochondral skeleton. Development *131*, 1309–1318.

Maeda, Y., Hojo, H., Shimohata, N., Choi, S., Yamamoto, K., Takato, T., Chung, U.I., and Ohba, S. (2013). Bone healing by sterilizable calcium phosphate tetrapods eluting osteogenic molecules. Biomaterials *34*, 5530–5537.

Marks, H., Kalkan, T., Menafra, R., Denissov, S., Jones, K., Hofemeister, H., Nichols, J., Kranz, A., Stewart, A.F., Smith, A., and Stunnenberg, H.G. (2012). The transcriptional and epigenomic foundations of ground state pluripotency. Cell *149*, 590–604.

Martí, E., and Bovolenta, P. (2002). Sonic hedgehog in CNS development: one signal, multiple outputs. Trends Neurosci. *25*, 89–96.

Nizzardo, M., Simone, C., Falcone, M., Locatelli, F., Riboldi, G., Comi, G.P., and Corti, S. (2010). Human motor neuron generation from embryonic stem cells and induced pluripotent stem cells. Cell. Mol. Life Sci. *67*, 3837–3847.

Ohba, S., Ikeda, T., Kugimiya, F., Yano, F., Lichtler, A.C., Nakamura, K., Takato, T., Kawaguchi, H., and Chung, U.I. (2007a). Identification of a potent combination of osteogenic genes for bone regeneration using embryonic stem (ES) cell-based sensor. FASEB J. *21*, 1777–1787.

Ohba, S., Nakajima, K., Komiyama, Y., Kugimiya, F., Igawa, K., Itaka, K., Moro, T., Nakamura, K., Kawaguchi, H., Takato, T., and Chung, U.I. (2007b). A novel osteogenic helioxanthin-derivative acts in a BMP-dependent manner. Biochem. Biophys. Res. Commun. *357*, 854–860.

Okabe, M., Ikawa, M., Kominami, K., Nakanishi, T., and Nishimune, Y. (1997). 'Green mice' as a source of ubiquitous green cells. FEBS Lett. *407*, 313–319.

Phillips, B.W., Belmonte, N., Vernochet, C., Ailhaud, G., and Dani, C. (2001). Compactin enhances osteogenesis in murine embryonic stem cells. Biochem. Biophys. Res. Commun. *284*, 478–484.

Plaisant, M., Fontaine, C., Cousin, W., Rochet, N., Dani, C., and Peraldi, P. (2009). Activation of hedgehog signaling inhibits osteoblast differentiation of human mesenchymal stem cells. Stem Cells *27*, 703–713.

Rodda, S.J., and McMahon, A.P. (2006). Distinct roles for Hedgehog and canonical Wnt signaling in specification, differentiation and maintenance of osteoblast progenitors. Development *133*, 3231–3244.

St-Jacques, B., Hammerschmidt, M., and McMahon, A.P. (1999). Indian hedgehog signaling regulates proliferation and differentiation of chondrocytes and is essential for bone formation. Genes Dev. *13*, 2072–2086.

Tai, G.P., Polak, J.M., Bishop, A.E., Christodoulou, I., and Buttery, L.D.K. (2004). Differentiation of osteoblasts from murine embryonic stem cells by overexpression of the transcriptional factor osterix. Tissue Eng. *10*, 1456–1466.

Tang, C., Lee, A.S., Volkmer, J.P., Sahoo, D., Nag, D., Mosley, A.R., Inlay, M.A., Ardehali, R., Chavez, S.L., Pera, R.R., et al. (2011). An antibody against SSEA-5 glycan on human pluripotent stem cells enables removal of teratoma-forming cells. Nat. Biotechnol. *29*, 829–834.

Tu, X., Joeng, K.S., and Long, F. (2012). Indian hedgehog requires additional effectors besides Runx2 to induce osteoblast differentiation. Dev. Biol. *362*, 76–82.

Wang, Y., Zhou, Z., Walsh, C.T., and McMahon, A.P. (2009). Selective translocation of intracellular Smoothened to the primary cilium in response to Hedgehog pathway modulation. Proc. Natl. Acad. Sci. USA *106*, 2623–2628.

Ye, J.H., Xu, Y.J., Gao, J., Yan, S.G., Zhao, J., Tu, Q., Zhang, J., Duan, X.J., Sommer, C.A., Mostoslavsky, G., et al. (2011). Critical-size calvarial bone defects healing in a mouse model with silk scaffolds and SATB2-modified iPSCs. Biomaterials *32*, 5065–5076.

Ying, Q.L., Wray, J., Nichols, J., Batlle-Morera, L., Doble, B., Woodgett, J., Cohen, P., and Smith, A. (2008). The ground state of embryonic stem cell self-renewal. Nature *453*, 519–523.

Zhang, X., Peterson, K.A., Liu, X.S., McMahon, A.P., and Ohba, S. (2013). Gene regulatory networks mediating canonical Wnt signal-directed control of pluripotency and differentiation in embryo stem cells. Stem Cells *31*, 2667–2679.

zur Nieden, N.I., Kempka, G., and Ahr, H.J. (2003). In vitro differentiation of embryonic stem cells into mineralized osteoblasts. Differentiation *71*, 18–27.